Structure of the second valence band in PbTe†

H. Sitter, K. Lischka, and H. Heinrich
Lehrkanzel für Experimentalphysik II, Universität Linz, Austria
(Received 28 February 1977)

The orientation of the main axis of the constant-energy ellipsoids and the mass-anisotropy ratio m_l/m_t of the secondary valence-band extrema of PbTe has been determined experimentally. These extrema are generally believed to be located at the Σ point of the Brillouin zone. Investigation of the anisotropy behavior of the coefficient of the conductivity of warm holes and magnetoresistance measurements showed that the main axes of these ellipsoids are parallel to $\langle 100 \rangle$ and do not coincide with the symmetry direction of the Σ point. The value of the mass-anisotropy ratio for the secondary valence band in PbTe is approximately 10. It has been derived from magnetoresistance experiments.

I. INTRODUCTION

The band structure of PbTe has been treated in the past in a series of theoretical and experimental papers. A review of these papers is given in Ref. 1. The following properties of the band structure of PbTe near the band edge have been found: (a) the valence-band edge $VB(L)$ and the conduction-band edge $CB(L)$ are both situated at the L point of the Brillouin zone[2-4]; (b) the surfaces of constant energy of $CB(L)$ and $VB(L)$ are ellipsoids with the main axis in a $\langle 111 \rangle$ direction[5]; (c) from experimental investigations of the fundamental absorption[6] and the Hall effect[7-10] as a function of lattice temperature, it has been suggested that there is a second set of maxima in the valence band of PbTe. Band-structure calculations showed[11,12] that these maxima are situated on the Σ direction of the Brillouin zone. We will call them $VB(\Sigma)$ therefore. These maxima lay approximately 0.17 eV below the valence-band edge $VB(L)$ at a lattice temperature of 0 K.[13] With increasing temperature the energetic separation of $VB(L)$ and $VB(\Sigma)$ decreases. At a lattice temperature of approximately 450 K both bands lay at the same energy.[6,7] At this temperature $VB(L)$ and $VB(\Sigma)$ are both populated by holes and contribute to the current conduction. Because of the high lattice temperature at which these maxima become populated, Shubnikov–de Haas and de Haas–van Alphen as well as cyclotron-resonance experiments could be carried out only at very high magnetic fields if at all possible. No information was available concerning the shape of the surfaces of constant energy in k space, the orientation of the main axis of ellipsoids of constant energy, nor the coefficient of mass anisotropy of the $VB(\Sigma)$ maxima.

In a recent letter[14] we reported the determination of the orientation of the main axis of the ellipsoids of the constant-energy surfaces of $VB(\Sigma)$. By analyzing the anisotropy of the warm-electron conductivity the direction of the main axis was obtained to be parallel to $\langle 100 \rangle$ in k space. It is the purpose of this paper to describe in more detail the experimental procedure and the results of this investigation of the warm-electron anisotropic conductivity as well as the results of magnetoconductivity measurements.

The anisotropy of the coefficient of the conduction of warm holes in PbTe was determined in a temperature range between 77 and 400 K. This coefficient is usually called β.[15] The experiments showed a $\langle 100 \rangle$ orientation for $VB(\Sigma)$, giving the first experimental proof that the main axis of the ellipsoids of $VB(\Sigma)$ do not coincide with the Σ direction in the Brillouin zone. In the following, the orientation of the main axis of the ellipsoids of constant energy will be called "orientation" for simplicity.

Magnetoresistance experiments were carried out in the temperature range from 300 to 420 K. From these experiments the orientation of $VB(\Sigma)$ was determined in agreement with the results of the β measurements. The coefficient of the mass-relaxation-time anisotropy $K' = (m_l/m_t)(\tau_t/\tau_l)$ was also measured.

The results of these two experiments have been explained by a model for the valence band of PbTe in which the ellipsoids of $VB(\Sigma)$ are situated along the edges of a cube in the Brillouin zone, whose edges are parallel to the $\langle 100 \rangle$ direction.

Both experiments are only capable of determining the orientation of the main axis of the constant-energy ellipsoids. They do not give any information on the location of their centers in k space. We therefore use the results from band-structure calculations,[11,12] which show that the second-valence-band extrema are located at Σ; we will construct a second-valence-band model based on this assumption. We would like to point out, however, that the experimental results are compatible with

ellipsoids centered at Σ as well as ellipsoids centered on X.

II. THEORY

A. Conductivity of warm carriers in semiconductors

The theory of the conductivity of warm carriers in semiconductors has been presented by Schmidt-Tiedemann[15] and will be outlined here briefly.

In semiconductors the mobility of carriers is given by

$$\mu_0 = e\tau_m(\langle\epsilon\rangle)/m^* . \tag{1}$$

τ_m stands for the momentum relaxation time, μ_0 for the mobility of the carriers at small electric field strength E, m^* is the effective mass, and $\langle\epsilon\rangle$ the mean energy of the carriers. If one expands μ into powers of $\langle\epsilon\rangle$ and assumes energy balance for the carrier gas one gets

$$\mu = \mu_0 + \frac{e}{m^*}\frac{d\tau}{d\langle\epsilon\rangle} m^* e\mu_0 E^2 \tau_\epsilon . \tag{2}$$

τ_ϵ is the energy relaxation time.

Now we can define β as

$$\beta = \frac{e^2}{m^*}\tau_\epsilon \frac{d\tau_m}{d\langle\epsilon\rangle} \tag{3}$$

and Eq. (2) can be written

$$\mu = \mu_0(1+\beta E^2) . \tag{4}$$

β is called the coefficient of the conductivity of warm carriers. In semiconductors where the constant-energy surfaces are ellipsoids of revolution, the effective mass and the conductivity are described by tensors. The current density j as function of the electric field strength E is given by

$$j_i = E\sigma_0 e_i + E^3\sigma_{iklm} e_k e_l e_m . \tag{5}$$

σ_{iklm} is the conductivity tensor, j_i is the ith component of the current density, and e_k, e_l, e_m are the directional cosine for the direction of E. Coordinate axes are parallel to the main crystallographic axes. For cubic-face-centered crystal systems the conductivity tensor can be simplified[16] and Eq. (5) can be written

$$j_i = \sigma_0 E e_i [1+\beta E^2 - \gamma E^2(e_j^2 + e_k^2)], \quad i\neq j\neq k\neq i . \tag{6}$$

Comparing Eqs. (4) and (6) one gets β as a function of the direction of the electric field

$$\beta(e_1, e_2, e_3) = \beta_0 + \gamma(\Sigma e_i^4 - 1) . \tag{7}$$

For E in a (100) plane Eq. (7) can be written in the form

$$\beta(\theta) = \beta_0 - 2\gamma \sin^2\theta\cos^2\theta , \tag{8}$$

where θ is the angle between E and a $\langle 100\rangle$ direction. The band structure of the semiconductor is included in Eq. (8) via the coefficient γ. γ depends on the orientation of the main axis of the ellipsoids of constant energy. γ has been calculated by Schmidt-Tiedemann[16] for ellipsoids with the main axis parallel to a $\langle 100\rangle$ direction (X orientation) and parallel to a $\langle 111\rangle$ direction (L orientation).

$$\gamma_X = \tfrac{3}{2}[(K-1)^2/(K+1)^2]\beta_{\langle 111\rangle} , \tag{9}$$

$$\gamma_L = -[2(K-1)^2/(2K+1)^2]\beta_{\langle 100\rangle} . \tag{10}$$

K is the mass-anisotropy factor m_l/m_t. For valleys with the main axis parallel to $\langle 110\rangle$ orientation (Σ valleys), γ is given by Ref. 14.

$$\gamma_\Sigma = -[(K-1)^2/2(3K^2+2K+1)]\beta_{\langle 100\rangle} . \tag{11}$$

From Eqs. (8)–(11) one gets an expression of $\beta(\theta)$ for the various band structures. The expression $\beta(45°)/\beta(0°)$ is larger than 1 for maxima with main axes parallel to $\langle 111\rangle$ and $\langle 110\rangle$ directions. For those with $\langle 100\rangle$ orientation $\beta(45°)/\beta(0°)$ is smaller than 1.

In the temperature range of interest for the present case, electron and hole scattering in PbTe is dominated by acoustic-phonon scattering and by polar optical-phonon scattering.[17] $\beta_{\langle 100\rangle}$ as function of lattice temperature is given for acoustic-phonon scattering[18] by

$$\beta_{ac} = (\mu-\mu_0)/\mu_0 E^2 = -0.147(\mu_0/u_1)^2 . \tag{12}$$

μ_0 is the mobility in the ohmic region and u_1 is the sound velocity.

For polar optical-phonon scattering β is given for temperatures above the Debye temperature[19] by

$$\beta_{po} = -\frac{m\mu_0^2}{k_B\Theta}\frac{[K_2(z)-K_1(z)][K_2(z)+4zK_1(z)]}{6zK_1(z)K_2(z)} , \tag{13}$$

where k_B is the Boltzmann constant, Θ the Debye temperature, K_1, K_2 are modified Bessel functions, and $z = \Theta/2T$.

The values of $\beta(0°)/\mu_0^2$ in PbTe for the different scattering mechanisms are plotted as dashed lines in Fig. 1. They were calculated by assuming the well-established relation $\mu_0(T) = (T_0/T)^{2\cdot 5}\mu_0(T_0)$. Σ and L indicate that conduction in the Σ, respectively, L band alone is assumed. The full curve in Fig. 1 has been calculated taking equal contribution to the conductivity by acoustic and polar optical scattering and a relative population of $VB(\Sigma)$ versus temperature which is plotted in Fig. 7. The parameters used for this calculation are listed in Table I. The dots are experimental data.

B. Magnetoresistance

The theory of magnetoresistance in semiconductors has been treated in the literature extensively.[20] It has been shown that the relative change of the specific resistance due to an applied magnetic field

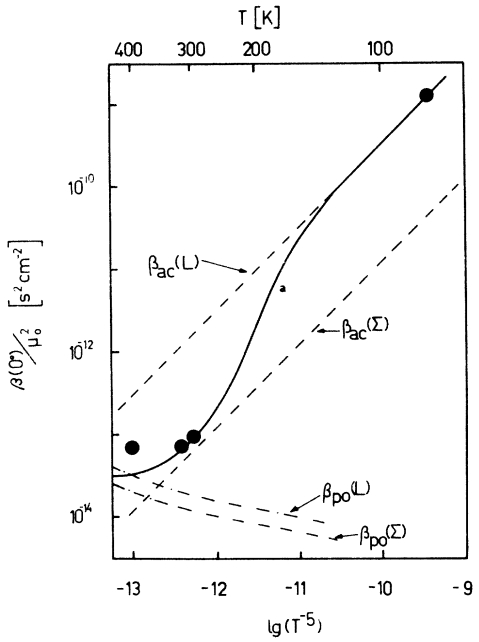

FIG. 1. Calculated values of β_0/μ_0^2 as a function of T. Dashed lines are calculated for acoustic-phonon (ac) and polar optical-phonon (po) scattering of carriers in $VB(L)$ and in $VB(\Sigma)$, respectively. The full curve has been calculated by assuming tentatively an equal contribution to the conductivity by ac. and po. scattering and taking the relative population of $VB(\Sigma)$ as shown in Fig. 7. Dots are experimental data.

can be expressed in the form

$$\Delta\rho/\rho = M^{s_1 s_2 s_3}_{r_1 r_2 r_3} \mu^2 H^2 , \tag{14}$$

where $M^{s_1 s_2 s_3}_{r_1 r_2 r_3}$ is the coefficient of magnetoresistance. $s_1 s_2 s_3$ is a vector parallel to the direction of the magnetic field $\vec{B}$ and $(r_1 r_2 r_3)$ is a vector parallel to the electric field $\vec{E}$. For a given direction of magnetic and electric field, M can be expressed as a linear combination of the Seitz coefficients b, c, d in cubic-face-centered crystals.[21,22]

$$M^{s_1 s_2 s_3}_{r_1 r_2 r_3} = b + c\left(\sum \tilde{r}_j \tilde{s}_j\right)^2 + d\sum \tilde{r}_j^2 \tilde{s}_j^2 ; \tag{15}$$

$\tilde{r}_1 \tilde{r}_2 \tilde{r}_3$ and $\tilde{s}_1 \tilde{s}_2 \tilde{s}_3$ are the directional cosines of the electric and magnetic field. The linear combination $z = -(b+c)/d$ is characteristic for the direction of the main axis of the ellipsoids of constant energy.[23] The values for z and some other linear combinations of b, c, d are listed in Table II for bands with ⟨100⟩, ⟨110⟩, and ⟨111⟩ orientation. Magnetoresistance for two-band conduction has been treated by Glicksman.[24] He derived an integral expression for the Seitz coefficients if conduction occurs in ⟨100⟩ and ⟨111⟩ bands. However the integrals can only be solved analytically for acoustic-phonon scattering. We therefore interpret

TABLE I. Parameters used for calculation of the population of $VB(\Sigma)$ and values of $\beta(0°)/\mu_0^2$.

$\Delta E_1(0) = 0.19$ eV
$\Delta E_2(0) = 0.17$ eV
$\frac{\partial \Delta E_1}{\partial T} = +4\times10^{-4}$ eV/K
$\frac{\partial \Delta E_2}{\partial T} = -4\times10^{-4}$ eV/K
$m_{VB(L)\,t} = 0.035 m_0$
$m_{VB(L)\,l} = 0.49 m_0$
$\frac{\partial \ln m_d^*(T)}{\partial \ln T} = 0.4$
$\mu_{VB(L)}/\mu_{VB(\Sigma)} = 4.3$
$\tau_l/\tau_t \simeq 3$ for $T > 150$ K

the effect of mixed conduction on the Seitz coefficients qualitatively. Two examples are given.

(i) Free carriers are transferred from a band with ⟨111⟩ orientation to a band with ⟨100⟩ orientation. At first z will be zero (see Table II). With increasing population of the ⟨100⟩ band the value of d will change its sign from plus to minus, and z will decrease to $-\infty$, jump to $+\infty$, and then decrease till it reaches +1.

(ii) Free carriers are transferred from a ⟨111⟩ band to a ⟨110⟩ band. In this case d does not change sign and z will slowly decrease with increasing population of the ⟨110⟩ bands from 0 to −1.

It is therefore possible to distinguish clearly between mixed ⟨111⟩ and ⟨100⟩ or ⟨111⟩ and ⟨110⟩ conduction when z is measured as a function of the population of the valleys.

A method for the determination of the anisotropy-relaxation-time factor K' without the explicit calculation of the Seitz coefficient for two-band conduction (⟨111⟩-⟨100⟩) is also given in Ref. 24. The linear combinations A and B are defined

$$A = (b+c)/(b+c+d) , \qquad B = (b+1)/(b+c+d) ; \tag{16}$$

with A and B a relation between the anisotropy-relaxation-time factor of both bands is given.

TABLE II. Values for the linear combinations of the Seitz coefficients for different orientations of the main axis of constant-energy ellipsoids.

Model	Linear combination	Sign (d)	$z = -(b+c)/d$
⟨100⟩	$b+c+d=0$	$d<0$	+1
⟨110⟩	$b+c-d=0$	$d>0$	−1
⟨111⟩	$b+c=0$	$d>0$	0

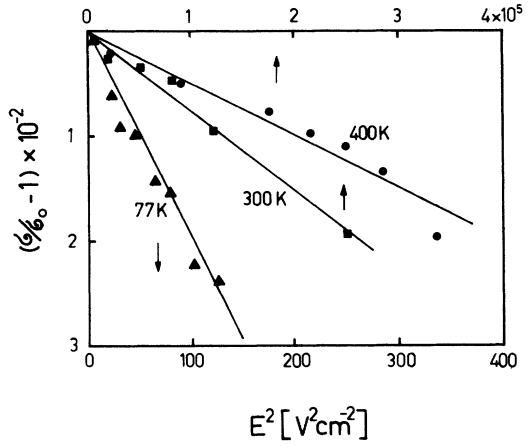

FIG. 2. Typical values of $\sigma/\sigma_0 - 1$ vs E^2 for different lattice temperatures which are indicated in the figure.

$$B = \frac{2K'^2_{\langle 111\rangle} + 5K'_{\langle 111\rangle} + 2}{2(K'_{\langle 111\rangle} - 1)^2} + A\,\frac{K'^2_{\langle 100\rangle} + K'_{\langle 100\rangle} + 1}{(K'_{\langle 100\rangle} + 1)^2}\,,$$
$$K'_{\langle 111\rangle} = (m^l_{\langle 111\rangle}/m^t_{\langle 111\rangle})(\tau^t_{\langle 111\rangle}/\tau^l_{\langle 111\rangle})\,, \qquad (17)$$
$$K'_{\langle 100\rangle} = (m^l_{\langle 100\rangle}/m^t_{\langle 100\rangle})(\tau^t_{\langle 100\rangle}/\tau^l_{\langle 100\rangle})\,.$$

Equation (17) is independent of the scattering mechanism. For various populations of the bands one gets different pairs of A and B. When one inserts this pair of A and B into Eq. (17) a functional dependence of $K'_{\langle 111\rangle}$ on $K'_{\langle 100\rangle}$ is obtained. These functions have the form of hyperbolas when plotted in a diagram with the axes $K'_{\langle 111\rangle}$ and $K'_{\langle 100\rangle}$. From the point of intersection of these hyperbolas the values of $K'_{\langle 111\rangle}$ and $K'_{\langle 100\rangle}$ can be determined.

C. Experimental method

All experiments described in this paper have been carried out on monocrystalline p-PbTe films epitaxially grown on a (100) plane of NaCl substrates.[25] Two directions for the current were possible: [100] and [110]. The samples were dumbbell shaped and had two potential probes each. The samples for magnetoresistance measurements had another probe on the opposite side for Hall-effect measurements. In the case of warm electrons the carrier concentration in the film was determined before etching the sample shape. The experiments and the results of the β measurements have been described in a recent letter.[14]

The resistivity of the samples as a function of electric field strength was measured by means of a Wheatstone bridge with current pulses of 200-nsec duration. The samples were placed in a cryostat which allowed measurements between 77 and 400 K. The measured resistivity was inverted to the conductivity $\sigma(E)$ as a function of the electric field strength. The change of the conductivity $\Delta\sigma(E)_{\text{exp}}$ has two physical reasons: (i) $\Delta\sigma(E)_w$ is the change of conductivity due to "warm carrier" effects and (ii) $\Delta\sigma(E)_h$ is due to Joule heating by the current pulse. At lattice temperatures in the range of room temperature, $\Delta\sigma(E)_w$ and $\Delta\sigma(E)_h$ are of the same order of magnitude in PbTe. Therefore a correction of $\Delta\sigma(E)_{\text{exp}}$ had to be made. Adiabatic heating of the sample was assumed and $\Delta\sigma(E)_h$ calculated, which was then subtracted from $\Delta\sigma(E)_{\text{exp}}$ to obtain $\Delta\sigma(E)_w$. The values of $[\sigma(E)_w/\sigma(0)] - 1$ were plotted versus E^2. In the range of warm-carrier conduction this gives a line with an inclination equal to β. As an example some of these results are shown in Fig. 2.

The experimental set up for magnetoresistance measurements was the usual one. The cryostat with the sample was placed between the poles of an electromagnet and could be rotated round an axis normal to the magnetic field lines. The sample axis was parallel to [110]. Two series of resistance measurements were carried out with each sample. (a) The axis of rotation parallel to the sample-direction. (b) The axis of rotation perpendicular to the sample direction. The geometric configuration for both series of measurements are shown in Figs. 3(a) and 3(b). Before the magnetoresistance measurements, the Hall effect was measured on each sample. The magnetoresistance

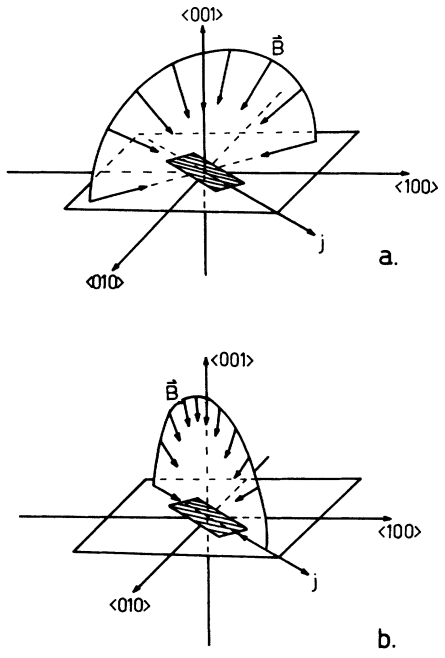

FIG. 3. Geometric configuration of magnetic field $\vec{B}$ and current $\vec{j}$ used for two different sets of magnetoresistance measurements.

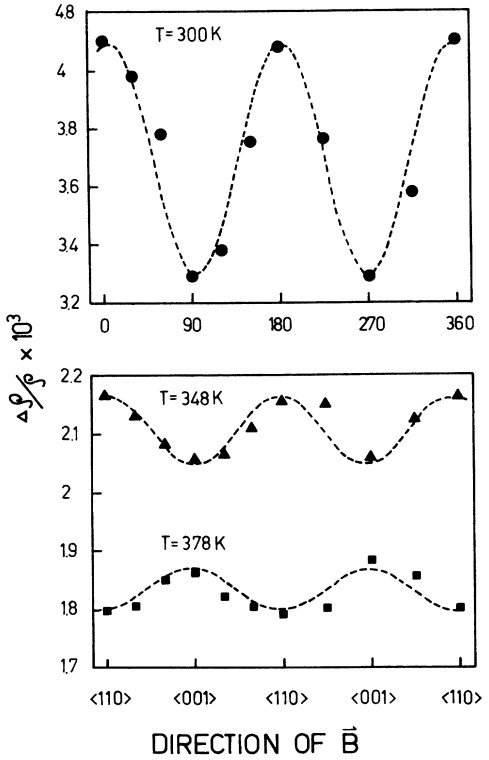

FIG. 4. Relative change of specific resistance ρ as function of the direction of the magnetic field $\vec{B}$ for various lattice temperatures measured on sample A. Dots are experimental values. The curves have been plotted as a guide for the eye. A change of the form of the curves is obtained between $T = 359$ and $T = 390$ K.

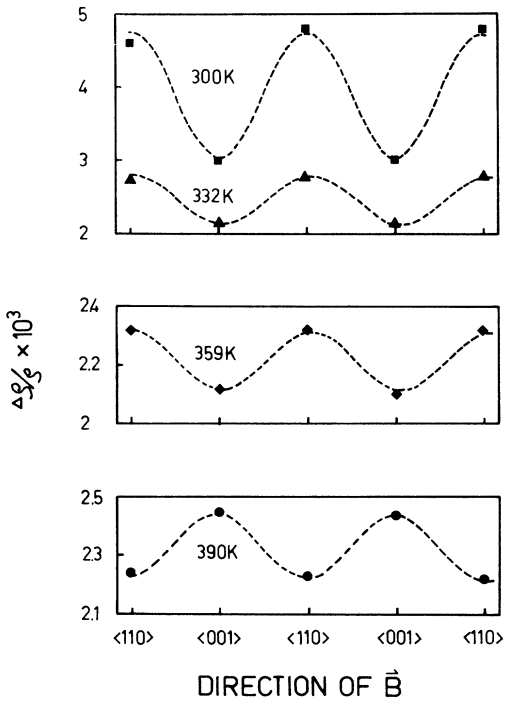

FIG. 5. See Fig. 4 caption.

at high temperatures is relatively small. In order to improve the accuracy of the measurements a computer was used on line to evaluate the data and to reduce the statistical fluctuations by performing two measurements per second and averaging them. Results of $\Delta\rho(B)/\rho_0$ versus the angle ϑ for sample A ($p = 2.7\times10^{17}$ cm^{-3}) and B ($p = 3.5\times10^{17}$ cm^{-3}) are shown in Figs. 4 and 5. ϑ is the angle between the direction of magnetic field B and the (100) plane. Each point in Figs. 4 and 5 has been obtained by averaging over approximately 250 individual measurements.

III. DISCUSSION

From data of the fundamental absorption[6] it is known that the energy gap of PbTe is approximately 0.19 eV at 0 K. It increases as lattice temperature increases. The temperature coefficient is approximately 4.1×10^{-4} eV/K. At temperatures higher than 450 K the gap becomes nearly constant. The interpretation for this behavior has been given in Ref. 8.

In PbTe a second valence band $VB(\Sigma)$ exists which lays energetically below the first valence band $VB(L)$ at 0 K. The energy gap between $VB(\Sigma)$ and the conduction band is nearly temperature independent and is approximately 0.36 eV. The energetic position of the bands of PbTe as a function of the lattice temperature is given in Fig. 6. When

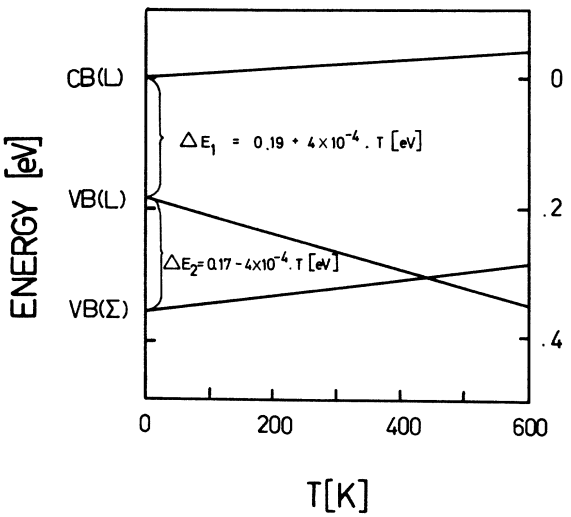

FIG. 6. Energetic location of the conduction band $CB(L)$ and valence band $VB(L)$ and of the second valence band $VB(\Sigma)$ in PbTe as a function of lattice temperature T.

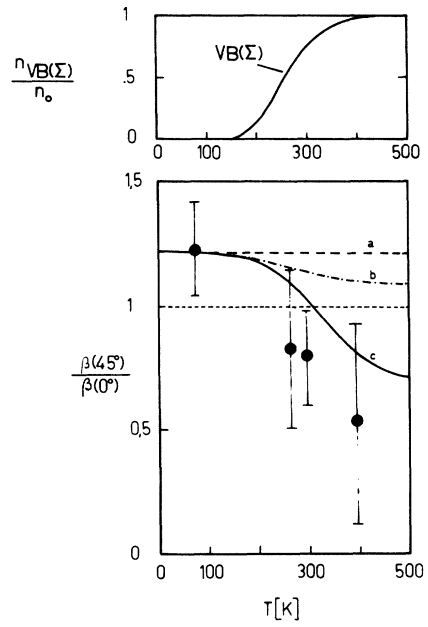

FIG. 7. $\beta(\theta=45°)/\beta(\theta=0°)$ and the population of $VB(\Sigma)$ as function of temperature. Dots are experimental results. Curves (a), (b) and (c) were calculated with a two-band model. Orientation of $VB(\Sigma)$ is ⟨111⟩ for (a), ⟨110⟩ for (b), and ⟨100⟩ for (c). Only in the case of (c) a ratio of $\beta(45°)/\beta(0°)$ smaller than 1 is obtained.

the lattice temperature reaches 450 K both bands have the same energetic position. There exists no experimental evidence for the location of this band in the Brillouin zone. However band-structure calculations[11,12] locate the second valence band of PbTe on the Σ direction of the Brillouin zone. Experimental data for the second-valence-band maxima are only available at high temperatures and have been obtained by investigation of the fundamental absorption.[6]

Extrapolation for $T \to 0$ however gives the same energetic position for this maxima and for the Σ maxima of band-structure calculations. We therefore adapt the notation $VB(\Sigma)$ for the second valence band. From Hall-effect measurements as a function of the temperature the effective mass of holes in $VB(\Sigma)$ has been determined. Its value is given in the literature in the range from $m^* = 0.6m_0$ to $1.4m_0$.[7,8,26,27] In Fig. 7 the experimentally determined values of $\beta(45°)/\beta(0°)$ are plotted as function of the lattice temperature. At temperatures above 300 K the ratio $\beta(45°)/\beta(0°)$ is smaller than 1. As shown in Sec. II this indicates that current is transported in a band consisting of ellipsoids with the main axis parallel to a ⟨100⟩ direction. For comparison the curves in Fig. 7 have been calculated assuming three different orientations for the second valence band. The best fit and also more important, the only curve which explains values smaller than 1 for $\beta(45°)/\beta(0°)$ is obtained with the ⟨100⟩ orientation for $VB(\Sigma)$. Also shown in Fig. 7 is the population of $VB(\Sigma)$ as function of T. For the calculation nonparabolicity of valence bands has been considered. The model for nonparabolicity was that presented by Cohen.[28] The parameters which were used for the calculation are listed in Table I.

The linear combination of the Seitz coefficient z, derived from experimental data of magnetoresistance as function of temperature is plotted in Fig. 8. In this figure the population of $VB(\Sigma)$ is indicated also. The change of sign in d occurs at rather high populations of $VB(\Sigma)$. This can be explained by the fact that magnetoresistance is proportional to μ^2 and $\mu_{VB(\Sigma)}/\mu_{VB(L)}$ is approximately 4.[10] As shown in Sec. II the form of z vs T is typically for the transition from conduction in ⟨111⟩-orientated ellipsoids to conduction in ⟨100⟩-orientated ellipsoids. From both experiments, warm-carrier conduction and magnetoresistance, it can be concluded that the structure of the valence band of PbTe can be described by a set of ellipsoids at the L point of the Brillouin zone with the main axis parallel to ⟨111⟩ directions and a second set of ellipsoids probably centered at a Σ point and

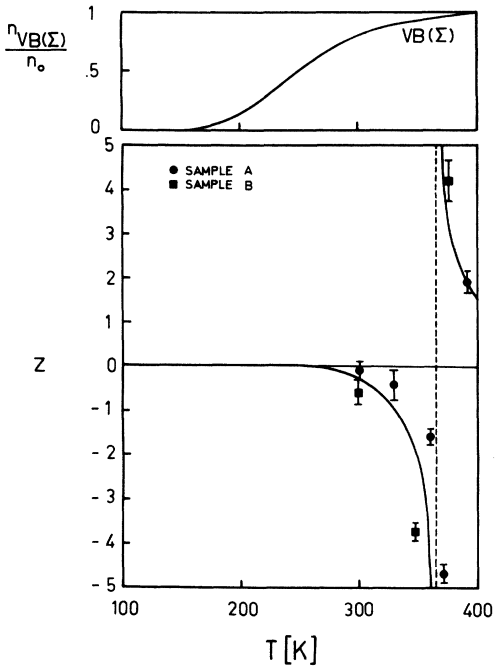

FIG. 8. Magnetoresistance symmetry parameter z vs T. Dots are experimental values. Curves are fitted to the experimental values. Dashed lines show where the change of sign of z occurs. In the upper diagram the calculated population of $VB(\Sigma)$ vs T is plotted.

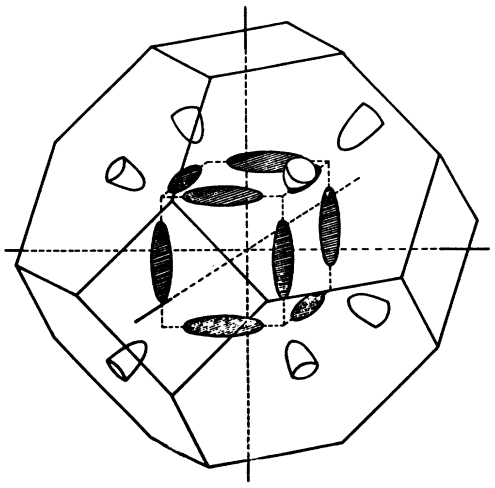

FIG. 9. Model for the constant-energy surface of the valence bands of PbTe, based on the experimental fact that for the second-valence-band extrema the main axis of the ellipsoids of constant energy are parallel to ⟨100⟩ and based on the result of band-structure calculations which show that these extrema are located at Σ.

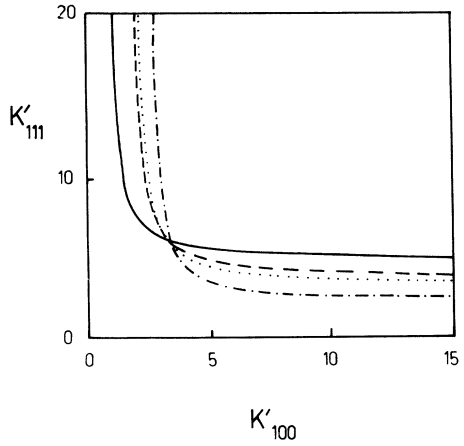

FIG. 10. Values of $K'_{\langle 111\rangle}$ vs $K'_{\langle 100\rangle}$ for different lattice temperatures T. The procedure to obtain the values of K' from magnetoresistance measurements is described in Sec. II.

the main axis parallel to ⟨100⟩ directions. This picture is somewhat similar to a model of the band structure of the valence band of SnTe presented by Allgaier.[29] The difference between Allgaier's model and ours is that we use a two-band model while Allgaier stated the existence of a strong nonparabolicity showing up as additive appendixes of the $VB(L)$ band in the k space. A model of the constant-energy surfaces of the valence bands of PbTe is given in Fig. 9.

The mass anisotropy ratio $K_{\langle 100\rangle}$ for holes in $VB(\Sigma)$ has been derived as described in Sec. II. In Fig. 10 $K'_{\langle 111\rangle}$ vs $K'_{\langle 100\rangle}$ is plotted for sample A for different temperatures (this means for different sets of b, c, d). The curves intersect at $K'_{\langle 111\rangle} = 5.5\pm1$ and $K'_{\langle 100\rangle} = 3.5\pm0.5$. For sample B similar results are obtained. This appears to be the first experimental determination of $K'_{\langle 100\rangle}$ for $VB(\Sigma)$ in PbTe. The value of $K'_{\langle 111\rangle}$ obtained is in good agreement with data obtained earlier on PbTe.[29] With $K'_{\langle 100\rangle}$ the mass-anisotropy ratio $K = m_l/m_t$ can be calculated when τ_t/τ_l is known. Herring and Vogt[30] showed that for acoustic-phonon scattering τ_t/τ_l does not depend on K and is approximately 1. For polar phonon scattering τ_t/τ_l depends strongly on K.[31] In PbTe the Debye temperature is approximately 150 K. Therefore polar optical scattering has to be considered as a strong-scattering mechanism at lattice temperatures above 300 K. This conclusion can also be drawn from Fig. 1, where the experimental values of β are compared with values calculated for different scattering mechanisms. Assuming pure polar optical scattering and using the diagram of τ_t/τ_l vs K of Ref. 31 we obtain for $VB(L)$ $m_l/m_t = 18\pm4$ and for $VB(\Sigma)$ $m_l/m_t = 10\pm2$. In reality these values may be smaller because of acoustic-phonon scattering.

In conclusion we can say that the experimental data obtained by magnetoresistance measurements and conductivity of warm holes indicate a model for the second valence band in PbTe consisting of probably 12 ellipsoids with the main axis parallel to the ⟨100⟩ direction and a mass-anisotropy ratio of approximately 10.

ACKNOWLEDGMENTS

The authors wish to thank Dr. A. Lopez-Otero for preparing the PbTe samples and Professor S. Rabii for many stimulating discussions.

†Work supported by Fonds zur Förderung der wissenschaftlichen Forschung in Österreich.

[1]Yu. I. Ravich, B. A. Efimova, and J. A. Smirnov, *Semiconducting Lead Chalogenides* (Plenum, New York, 1970), pp. 118–122.
[2]Yu. I. Ravich, B. A. Efimova, and V. I. Tamarchenko, Phys. Status Solidi 43, 453.
[3]K. Shogenji and S. Uchiyama, J. Phys. Soc. Jpn. 12, 1164 (1957).
[4]R. S. Allgaier, Phys. Rev. 112, 828 (1958).
[5]Yu. I. Ravich, B. A. Efimova, and V. I. Tamarchenko, Phys. Status Solidi 43, 11 (1971).
[6]A. F. Gibson, Proc. Phys. Soc. B 65, 378ff (1952).
[7]A. A. Andreev and V. N. Radinov, Fiz. Tekh. Poluprovodn. 1, 183 (1967) [Sov. Phys.-Semicond. 1, 145 (1967)].
[8]R. S. Allgaier and B. B. Houston, J. Appl. Phys. 37, 302 (1966).

[9]N. V. Kolomoets, M. N. Vinogradova, L. M. Sysoeva, Fiz. Tekh. Poluprovodn. 1, 1222 (1968) [Sov. Phys.-Semicond. 1, 1020 (1968)].
[10]A. J. Crocher and L. M. Rogers, Br. J. Appl. Phys. 18, 563 (1967).
[11]J. W. Jung and M. L. Cohen, Phys. Rev. 180, 823 (1969).
[12]F. Hermann, R. L. Kortum, I. B. Ortenburger, and J. P. Van Dyke, J. Phys. (Paris) 29, C4-62 (1968).
[13]A. A. Andreev, J. Phys. (Paris) 29, C4-50 (1968).
[14]H. Heinrich, K. Lischka, H. Sitter, and M. Kriechbaum, Phys. Rev. Lett. 35, 1107 (1975).
[15]J. K. Schmidt-Tiedemann, Philips Res. Rep. 18, 338 (1963).
[16]K. J. Schmidt-Tiedemann, Phys. Rev. 123, 1999 (1961).
[17]Yu. I. Ravich, B. A. Efimova, and Y. I. Tamarchenko, Phys. Status Solidi 43, 433 (1971).
[18]K. H. Seeger, *Semiconductor Physics* (Springer, New York, 1973), p. 181.
[19]K. H. Seeger, *Semiconductor Physics* (Springer, New York, 1973), p. 217.
[20]R. A. Smith, *Semiconductors* (Cambridge U.P., Cambridge, 1968), p. 123.
[21]Frederick Seitz, Phys. Rev. 79, 372 (1950).
[22]G. L. Pearson and H. Suhl, Phys. Rev. 83, 768 (1951).
[23]R. S. Allgaier and B. B. Houston, Phys. Rev. B 5, 2186 (1972).
[24]Maurice Glicksman, Phys. Rev. 102, 1496 (1958).
[25]A. Lopez-Otero and L. D. Haas, Thin Solid Films 23, 1 (1974).
[26]S. V. Airapetyants, M. N. Vinogradova, I. N. Dubrovskaya, N. V. Kolomoets, and I. M. Rudnick, Fiz. Tverd. Tela 8, 1336 (1966) [Sov. Phys.-Solid State 8, 1069 (1966)].
[27]J. R. Dixon and H. R. Riedl, Phys. Rev. 138, A873 (1965).
[28]M. H. Cohen, Phys. Rev. 121, 387 (1961).
[29]R. S. Allgaier, in *Proceedings of the Fifth International Conference on Physics of Semiconductors, Prague, 1960* (Academic, New York, 1961), p. 1037.
[30]C. Herring and E. Vogt, Phys. Rev. 101, 944 (1956).
[31]O. S. Gryaznov and Yu. I. Ravich, Fiz. Tekh. Poluprovodn. 3, 1310 (1969) [Sov. Phys.-Semicond. 3, 1092 (1970)].